Controllable fabrication and electromechanical characterization of electrophoresis assembled single-walled carbon nanotube-polymer film transducers

Article *in* Microsystem Technologies · July 2012

DOI: 10.1007/s00542-012-1697-4

2 authors, including:

Dongzhi Zhang
China University of Petroleum - Beijing
97 PUBLICATIONS **1,322** CITATIONS

SEE PROFILE

Microsyst Technol (2013) 19:1041–1047
DOI 10.1007/s00542-012-1697-4

TECHNICAL PAPER

Controllable fabrication and electromechanical characterization of electrophoresis assembled single-walled carbon nanotube-polymer film transducers

Dongzhi Zhang · Tianhong Cui

Received: 28 August 2012 / Accepted: 15 November 2012 / Published online: 29 November 2012

Abstract This paper presents a controllable electrophoresis allowing a directed deposition of negatively charged single-walled carbon nanotubes (SWNTs) on an electro-active polymer to fabricate thin-film transducers under an electric field excitation. The assembled high-density SWNT networks are verified with SEM micrograph and Raman spectroscopy, and the electric filed-induced mechanism for electrophoresis of SWNT is investigated using electrochemical analysis technique. The dynamic electromechanical properties are characterized by a combinative approach of piezoelectric excitation and laser vibrometer measurement. A remarkable performance enhancement and tunability for such thin-film transducers in both resonant frequency and quality factor is demonstrated, compared with pure polymer. This observed enhancement can not only be exploited to tailor the thin-film transducers for desired electromechanical properties, but also create versatile pathways for variety of applications including polymeric electronic technologies.

1 Introduction

Many existing and emerging M/NEMS devices benefit from the building blocks of single-walled carbon nanotubes (SWNTs) since their discovery in 1991 by (Iijima 1991). This is not simply due to their nanoscale size but rather to their overall properties. SWNTs are extremely stiff and strong, demonstrating remarkable Young's modulus of up to 1 TPa and tensile strength over 60 GPa (Lourie and Wagner 1998; Treacy et al. 1996). Moreover, SWNTs have excellent electrical properties, exhibiting high thermal conductivities up to 3,500 W m^{-1} K^{-1} and high current-carrying capacities over 10^9 A cm^{-2} (Pop et al. 2006; Yao et al. 2000). However, despite an attractive potential of SWNTs, challenges in manipulating and positioning to achieve a control over self assembly still constitute the major obstacles towards scalable device applications (Vosgueritchian et al. 2010). Thin films of SWNTs as an attractive, emerging class of material, are readily suitable for scalable integration into next generation micro/nano devices including field-effect transistors, biochemical sensors, electro-active actuators, and ratio frequency (RF) switches, owing to their properties that can approach the exceptional electrical, mechanical, and optical characteristics of individual SWNTs (Cao and Rogers 2010; Baughman et al. 2002; Avouris et al. 2007). Some successful approaches for SWNT film preparation can be divided into two main categories involving solution-based deposition processes and chemical vapor deposition (CVD) growth (Huang et al. 2007). The solution-based techniques are attractive since they can be cost-effectively scaled to large areas and compatible with a wide variety of substrates, compared to CVD deposition method. As an alternative approach among them, electrical field-induced electrophoresis process, allowed for directed deposition of chemically functionalized SWNTs to form a highly-compact and homogeneous membrane with a molecular-level control over the architecture. The electrophoresis self-assembly approach offers a promising pathway to form

D. Zhang · T. Cui (✉)
Department of Mechanical Engineering,
University of Minnesota, 111 Church Street S.E.,
Minneapolis, MN 55455, USA
e-mail: tcui@me.umn.edu

D. Zhang
College of Information and Control Engineering,
China University of Petroleum (East China),
Qingdao 266580, China

SWNT films with good mechanical bonding as epitaxial deposition processes, and to yield excellent mechanical and electrical properties. Lu et al. (2009) reported directed assembly SWNT film with Young's modulus ranged from 350 to 830 GPa, and the electrical resistivity about 8.7 m Ω cm, exhibiting a promising application as a NEMS switch.

To achieve the full potential in SWNT-based devices, this paper presents a well-controllable electrophoresis for assembled single-walled carbon nanotube (SWNT)/polymer transducers under an electric field excitation. A kind of electro-active polymer, poly(vinylidene fluoride) (PVDF) film, with silver ink printed as electrodes, serves as a substrate for the SWNT deposition. The architecture of self-assembled SWNT films was controllable under a variation of electric field excitations. The electrical field-induced mechanism of the controllable assembly of SWNTs was investigated using electrochemical analysis technique. The directed assembled high-density SWNT networks were verified with SEM micrograph and Raman spectroscopy. The dynamic electromechanical properties are characterized by a combinative approach of piezoelectric excitation and laser vibrometer measurement. A remarkable performance enhancement for such thin-film transducers in both resonant frequency and quality factor is demonstrated, compared with pure polymer. This observed enhancement can not only be exploited to tailor the thin-film transducers for desired electromechanical properties, but also create versatile and promising pathways for next-generation actuators, sensors, and microsystems with a high performance.

2 Fabrication of SWNT/polymer transducer by electrophoresis

Pristine SWNTs (50 μm in length, 1.1 nm in diameter, and 2.1 g/cm^3 in density) were chemically functionalized with the concentrated acid (3:1 for 98 wt% H_2SO_4: 70 wt% HNO_3) at 110 °C and stirred at 140 rmp for 1 h, followed by 0.22 μm micropore membrane filtering and several rinsing by de-ionized water (DI water) until the supernatant had pH = 5 or more. The chemically treated SWNTs were negatively charged by covalently-attached carboxylic groups on the sidewalls as well as openings, which facilitated the uniformly well-dispersion of SWNTs into water with a concentration of 1 g/L approximately. Ag ink-coated poly(vinylidene fluoride) (PVDF) film from Measurement Specialties Inc. used as substrate, which consists of 52 μm PVDF film and 6 μm Ag ink-printed electrode on both sides. The substrate film was firmly bonded to a holed poly(methy1 methacrylate) (PMMA) support block for fabricating a free-standing anode membrane for electrophoresis process, and a copper patch exploited as its cathode. During the fabrication process of the SWNT/polymer transducers, first, chemically-treated SWNT suspension with concentration of 1 g/L was put into a glass vessel with the anode/cathode electrodes immersed in the solution vertically, and a DC power supply was applied to offer an electric field excitation. The electric fields applied, E subject to $E = U/d$, can be adjusted by the voltages, U and distances, d between the two electrodes. In our work the electric field intensity ranged from 1 to 4 V/cm, and the assembling duration was 30 min for each sample. Figure 1 illustrates the schematic diagram of fabrication process of an SWNT/PVDF thin-film transducer by electrophoresis assembly, consisting of functionalized SWNTs, Ag ink-coated PVDF substrate, and suspension-based electrophoresis assembly of an SWNT film. Figure 2a shows the self-assembly principle for SWNTs electrophoresis, negatively-charged SWNTs was polarized and actuated to move along the opposite direction of electric field gradient through imposing a spatial electric field, and eventually was assembled on the PVDF-based substrate. After fulfilling the SWNTs assembly, the film device was finally air dried at room temperature overnight to obtain purified SWNT film. The sketch before and after electrophoresis self-assembly and air drying was illustrated in Fig. 2b. A highly-compact and homogeneous membrane was bonding on the substrate through a molecular-level control over the architecture.

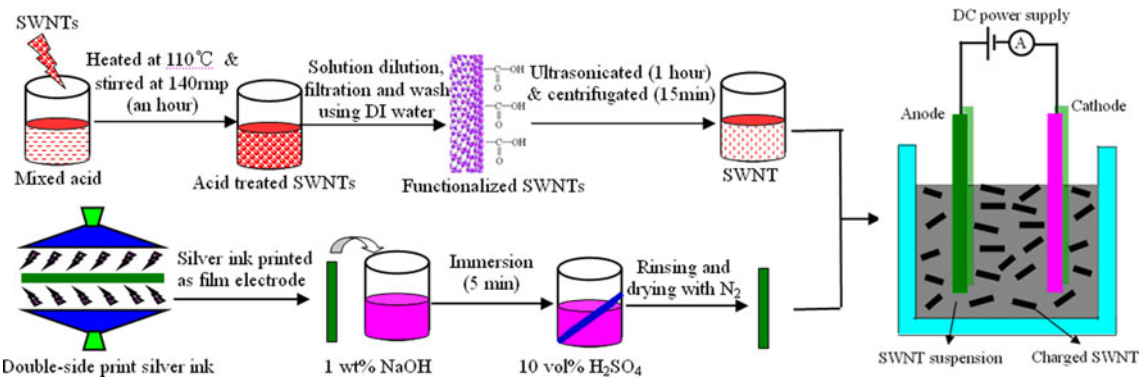

Fig. 1 Schematic of fabrication process of an SWNT/PVDF thin-film transducer by electrophoresis assembly

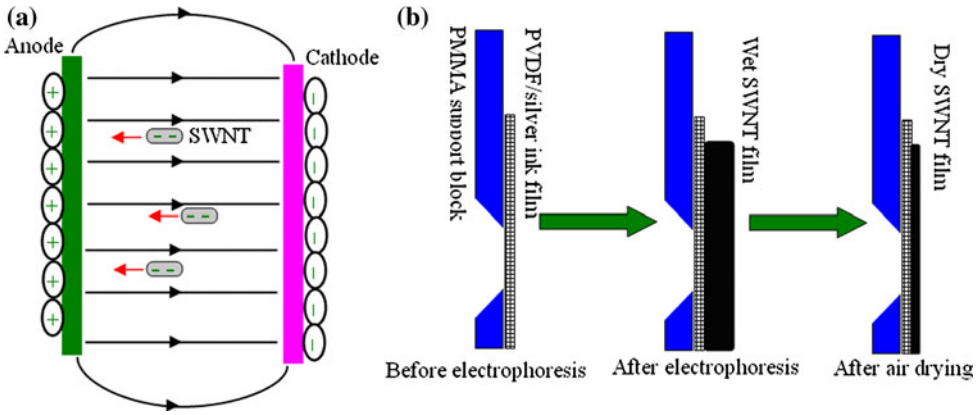

Fig. 2 **a** Electrophoresis self-assembly principle and **b** electrophoresis process of an SWNT film

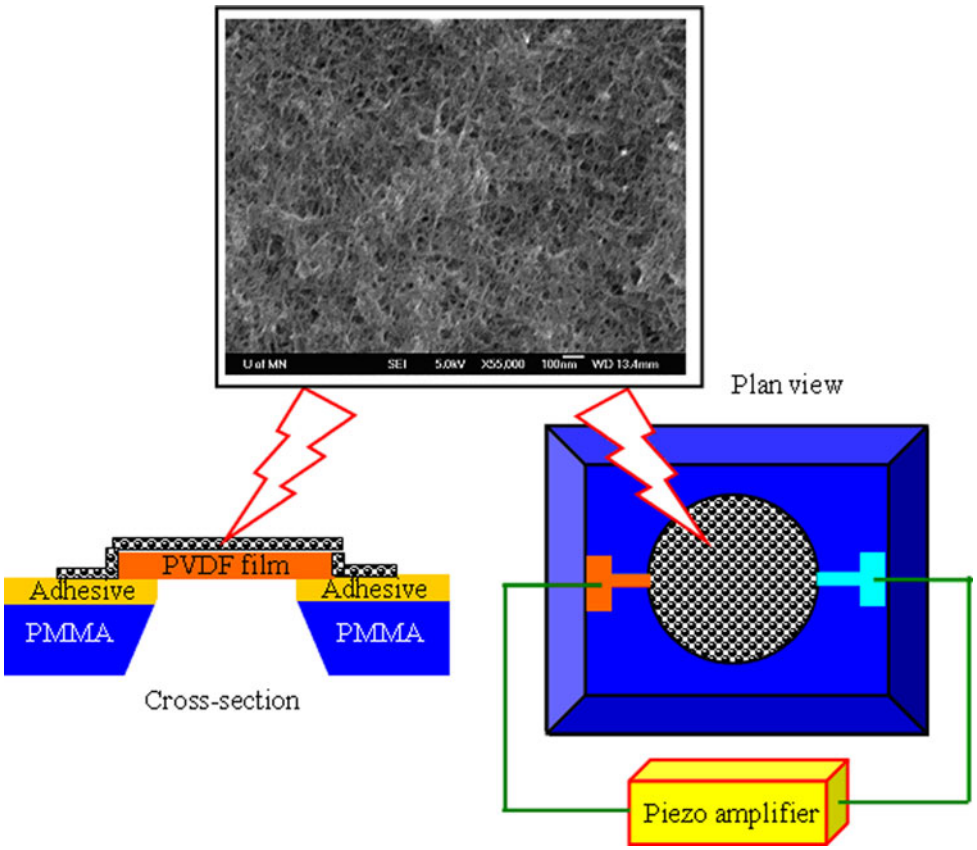

Fig. 3 Sketch of electrophoresis assembled SWNT/polymer film transducer, and surface morphology observed by SEM

Figure 3 shows the schematic diagram of direct assembled SWNT/polymer transducers along with the piezoelectric testing scheme.

3 Electrophoresis SWNTs film characterization

The surface morphology of the electrophoresis assembled SWNT film were inspected by scanning electron microscopy (SEM, JEOL 6700F), and the top-view SEM results were obtained at an acceleration voltage of 5 kV, as shown in Fig. 3. The individual SWNTs as well as their bundles are observed, and they form a high-densely, randomly entangled and cross-linked network structures with a good electrical contact.

Raman characterization on the electrophoresis assembled SWNT film was performed by Confocal Raman Microscope (alpha300R) at the wavelength of 514.45 nm and the power of 10 mW for 10 s, and the Raman spectrum is illustrated in Fig. 4. The main feature of the spectrum in SWNT film is the radial breathing mode (RBM) at 206 cm^{-1}, where all atoms of the SWNT vibrate radically in phase. It is widely known that RBM is dependent only on SWNT diameter through the following equation proposed by Graupner (2007):

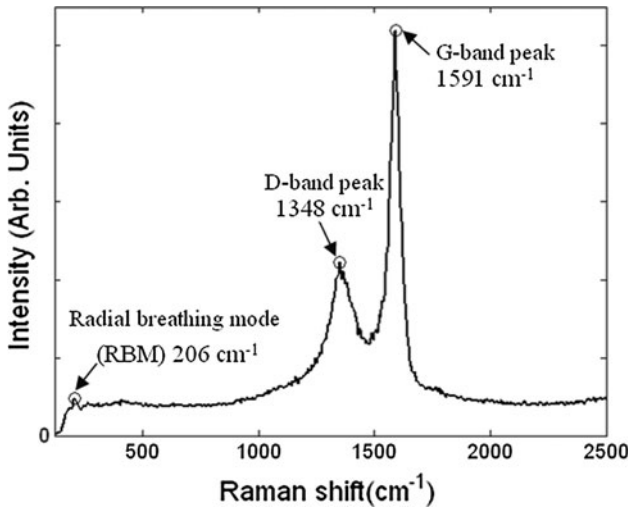

Fig. 4 Raman characterization of an electrophoresis assembled SWNTs film

$$\omega_{\mathrm{RBM}} = \frac{A}{d} + B \tag{1}$$

where ω is the wavenumber at RBM, d is the diameter of the SWNTs, and A and B are constants. Based on the reported values of $A = 204\ \mathrm{cm}^{-1}$ nm and $B = 27\ \mathrm{cm}^{-1}$ (Meyer et al. 2005), the diameter of SWNTs used in this study has been determined as 1.14 nm, which is in good agreement with the material data. The peak of disorder-induced band (D-band) at 1,348 cm^{-1} represented high-density and purity of chemically functionalized SWNTs assembled, and the relative strong intensity of the tangential mode (G-band) at 1,591 cm^{-1} indicated that the amount of residual ill-organized graphite (amorphous carbon) in the sample of SWNT was reached the negligible level (Liu et al. 2007; Belin and Epron 2005). All these characteristic of typical peaks demonstrated the presence of SWNTs in overall good quality and bonding state.

The electric-field-induced mechanism of the controllable assembly of SWNTs was investigated using a CHI 630 Electrochemical Analyzer, in which the current density and area specific resistance can be captured through the timely I–V measurement between the two electrodes during the electrophoretic self-assembly process. The proportional relationship between the current density and the electric field excitation is shown in Fig. 5a, which indicates that the current density linearly increases correspondingly with the increasing of electric field intensity. The curve slope 0. 433 mS/cm, which means electric conductivity of the SWNT solution, is measured. Figure 5b illustrates that the current density change as a function of electrophoresis duration under different fixed electrical field, and the inset shows the area special resistance as a function of electrophoresis duration. It can be seen from Fig. 5b that, the current density increases with the electric field intensity,

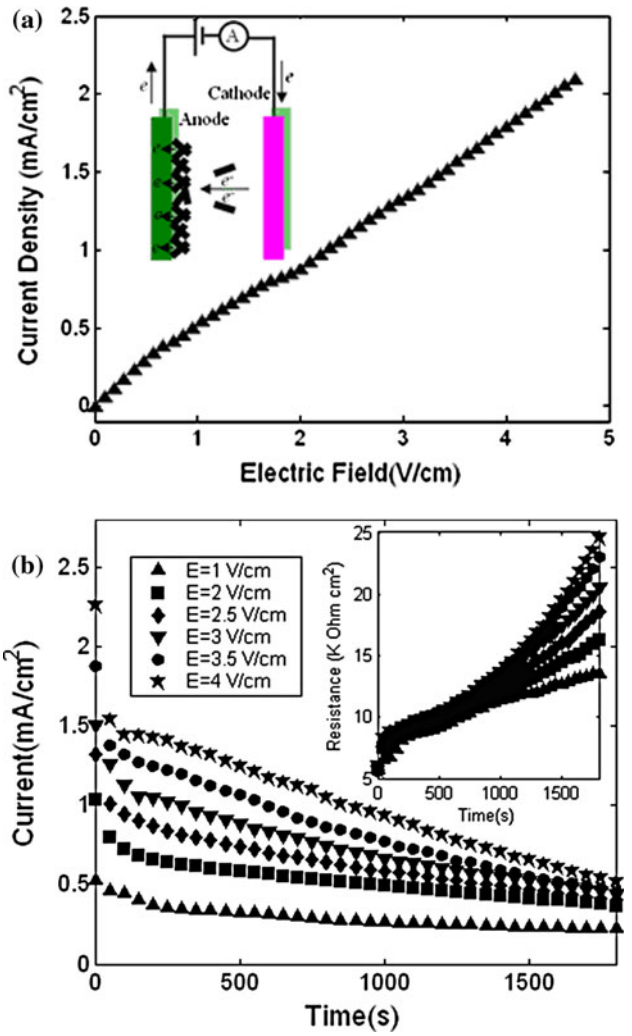

Fig. 5 Mechanism characterization of electrophoresis assembly with different electric field excitations; **a** Current density versus electric field, **b** current density change as a function of electrophoresis duration under different fixed electrical field

while follows a decrease with the electrophoresis duration. This can be interpreted as the fact that the electric conductivity of the SWNT solution reduces with the well-assembly of SWNTs during the electrophoresis process.

Thickness profile measurement was performed to the well-assembled SWNT films by a surface profilometer (Tencor P10). Figure 6 presents the step height profiles for SWNT films assembled under different electric field excitation for 30 min, the inset plots the average thickness of SWNT films versus electric field applied, and the error bars represent standard deviations of experimental data. The step heights of SWNT films from 0.29 to 1.92 μm were clearly found nearly proportional to the electric field applied between electrodes, from 1 to 4 V/cm, resulting in a variation of SWNT loading fraction from 0.45 to 2.91 vol.% in the whole composite films.

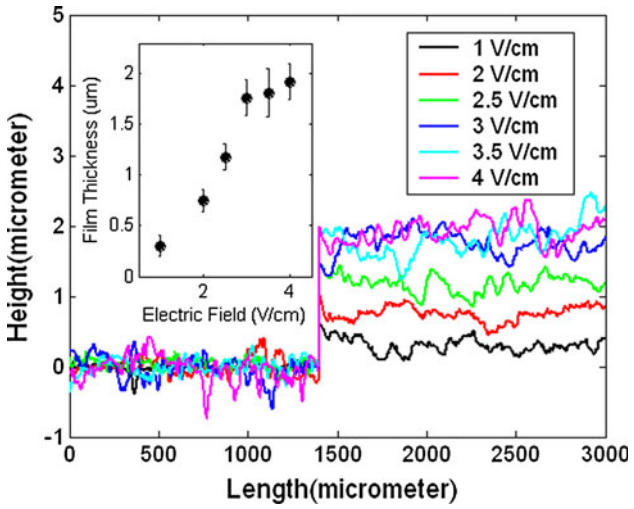

Fig. 6 Film height profile of assembled SWNT under different electric field excitations observed by profilometer

4 Performance characterization and discussion

The electromechanical SWNT/polymer thin film transducers were mechanically excited via the piezoelectric effect of electro-active polymer substrate by applying an AC voltage between the electrodes. This creates a strain along the radial of the circular membrane that develops into a bending moment resulting in mechanical resonance at the appropriate frequency of the AC voltage. The electromechanical SWNT/polymer thin film transducers can be modeled as a driven damped harmonic oscillator characterized by a time-dependent mass-spring equation given by

$$\ddot{z}(t) + \frac{2\pi f_0}{Q}\dot{z}(t) + (2\pi f_0)^2 z(t) = \frac{F_{\text{drive}}}{m_{\text{eff}}} \tag{2}$$

with z the displacement, $f_0 = \frac{1}{2\pi}\sqrt{\frac{k}{m_{\text{eff}}}}$ the mechanical resonance frequency, k the spring constant, m_{eff} the effective mass, $Q = f_0/\Delta f_{-3dB}$ the quality factor, and F_{drive} the oscillating driven force on the thin film transducers, is given by

$$F_{\text{drive}} = kA_{\text{drive}}^{\max}\cos(2\pi ft) \tag{3}$$

where $A_{\text{drive}}^{\max}$ is a coefficient related to electromechanical coupling at the resonate frequency, which can be gained from experimental test. For thin-film transducers with specific geometries, the resonant frequencies are determined only by the mechanical properties of the transducer and pre-tension, and are independent of the relative contribution of the electromechanically coupling. The fundamental frequencies of a circular thin-film clamped at the boundary under the contribution of stiffness-tension is given by Hong et al. (2008)

$$f_0 = \frac{1}{2\pi R}\sqrt{\frac{1}{\rho h}\left[\frac{\alpha_p^2}{R^2}D + \alpha_m^2 T\right]} \tag{4}$$

where $D = Eh^3/[12(1-v^2)]$ is the bending stiffness, T is the pre-tension, E, v, h, ρ are the Young's modulus, Poisson's ratio, thickness and density of the thin-film, α_p and α_m are the vibration constants. Without considering the pre-tension effect, the resonate frequency and spring constant for the circular thin-film transducer can be obtained as

$$f_0 = \frac{10.22h}{4\pi R^2}\sqrt{\frac{E}{3\rho(1-v^2)}} \tag{5}$$

$$k = \frac{8.704E\pi h^3}{R^2(1-v^2)} \tag{6}$$

The amplitude/phase-frequency response of the thin film transducer has a Lorentzian shap characterized using the harmonic oscillator model as

$$A = \frac{1}{(2\pi)^2}\frac{F_{\text{drive}}}{m_{\text{eff}}}\frac{1}{\sqrt{(f^2-f_0^2)^2 + \frac{f_0^2 f^2}{Q^2}}} = \frac{A_{\text{drive}}^{\max} f_0^2}{\sqrt{(f^2-f_0^2)^2 + \frac{f_0^2 f^2}{Q^2}}} \tag{7}$$

$$\tan\theta = \frac{ff_0/Q}{f_0^2 - f^2} \tag{8}$$

where A is the vibration amplitude and $\theta$the phase angle of the transducer system.

The dynamic electromechanical properties were characterized by a combinative approach of piezoelectric excitation and laser vibrometer measurement. A highly sensitive laser vibrometer was utilized to determine the resonance frequencies and Q factors resulted by the self-assembled of SWNT films. Figure 7 illustrates the schematics of experiment setup, consisting of a piezoelectric exciter (VF-500, DSM, LLC) and a laser-scanning vibrometer (PSV-400, Polytec). The laser measurement system and equipment are controlled by the vibrometer controller, and the testing samples are fixed on the vibration isolation platform. A sinusoidal harmonic excitation was applied to drive the carbon nanotube-PVDF electro-active film transducers, and the wavelength of He–Ne laser used is 633 nm. Once the samples are under test, the scanning excitation frequency was implied to the samples and the corresponding vibration amplitude could be optically captured by the photodetector and then transformed into electrical signal for processing by the computer data-acquisition system.

Figure 8 shows the contrast of amplitude-frequency curves determined for a pure polymer transducer and the electrophoresis self-assembled SWNT/polymer transducer (SWNT loading fraction at 2.68 vol.%) under different

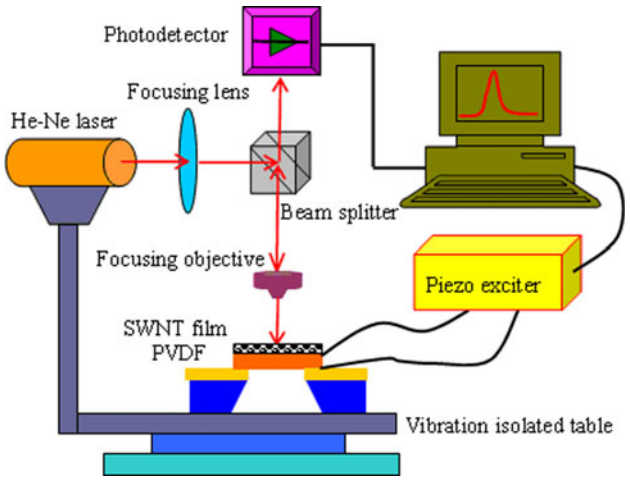

Fig. 7 Schematic of experimental setup for the measurement of frequency response

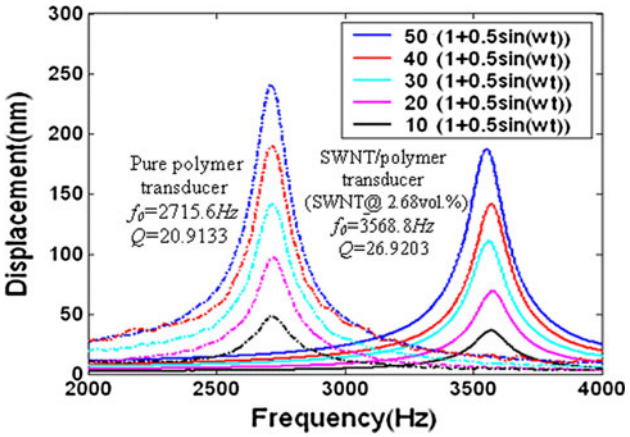

Fig. 8 Displacement-frequency curves determined for a pure polymer transducer and an SWNT/PVDF transducer (SWNT fraction at 2.68 vol.%) under different voltages applied

voltages applied. The vibration amplitude increases linearly with the increasing of excitation voltage applied. The resonance frequency was enhanced by 131.42 % from 2,715.6 to 3,568.8 Hz, and the quality factor Q was enhanced by 128.72 % from 20.9133 to 26.9203. To characterize the tunable dynamic electromechanical properties of an electrophoresis assembled SWNT film, we investigated a series of SWNT/polymer piezoelectric film transducers with a variation of SWNT loading fraction from 0.45 to 2.91 vol.%, resulted from the excitation of different electric-field intensities from 1 to 4 V/cm. The performance enhancement in resonance frequency and Q factor was characterized through experimental test by piezoelectric excitation and laser measurement. The performance enhancement ratio for all SWNT/polymer transducers plotted versus the variation of SWNT loading fraction is illustrated in Fig. 9. The lines show a linearly fitting to the measured data, and the correlation coefficients

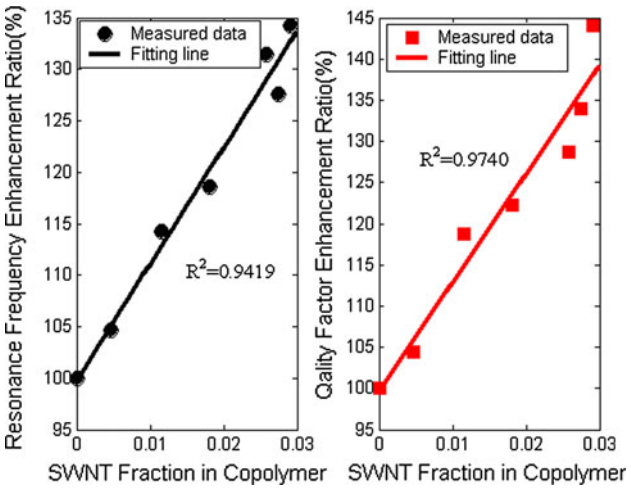

Fig. 9 Performance enhancement ratio in resonate frequency and quality factor for all SWNT/polymer transducers

are 0.9419 and 0.9740 for resonance frequency and Q factor, respectively. 135 % enhancement in both resonant frequency and quality factor of SWNT/polymer transducers with SWNT loading less than 3 vol.% is observed. As a result, over 10 times enhancement of resonant frequency and quality factor for transducers with an SWNT fraction at 80 vol.% is predicted through theoretical verification. Such remarkable enhancement results from the increased mechanical properties and spring constants through the SWNT loading in the electro-active polymer by electrophoresis. The combination of SWNTs with electro-active polymer represents an important step in the development of SWNT-based devices that may find utility in areas such as flexible electronics, next-generation high-performance thin-film devices with potential applications to various electromechanical systems.

5 Conclusion

Thin SWNT films, as an attractive and emerging material, are readily suitable for scalable integration into next generation micro/nano devices including field-effect transistors, biochemical sensors, and ratio frequency (RF) switches, owing to their exceptional electrical and mechanical properties. This work presents an electric-field-induced electrophoresis assembly for controllable deposition of functionalized SWNTs on electro-active polymer to fabricate thin-film transducers. The electrophoresis mechanism of the solution-based directed assembly of SWNTs under different electric field excitations was investigated using electrochemical analysis technique. The assembled high-density SWNT networks were verified with SEM micrograph and Raman spectroscopy. The dynamic electromechanical properties are characterized through

piezoelectric excitation and laser vibrometer measurement. 135 % enhancement in both resonant frequency and quality factor of SWNT/polymer transducers with SWNT loading less than 3 vol.% is observed. As a result, over 10 times enhancement of resonant frequency and quality factor for transducers with an SWNT fraction at 80 vol.% can be predicted, compared with pure polymer. Such remarkable enhancement results from the increased mechanical properties through high-density carbon nanotube random networks. This work can not only be exploited to tailor the thin-film transducers for desired electromechanical properties, but also to create versatile and promising pathways for next-generation actuators, sensors, and microsystems with a high performance.

Acknowledgments This work was partially supported by the Minnesota Partnership Program and the Promotive Research Foundation for the Excellent Middle-Aged and Youth Scientists of Shandong Province of China (No. BS2012DX044), and the Fundamental Research Funds for the Central Universities of China (No. 12CX04065A). We also acknowledge the Characterization Facility at the University of Minnesota. In particular, we thank Dr. Peng Li for the valuable discussion and help on the SEM characterization.

References

Avouris P, Chen Z, Perebeinos V (2007) Carbon-based electronics. Nat Nanotechnol 2:605–615

Baughman RH, Zakhidov AA, de Heer WA (2002) Carbon nanotubes-the route toward applications. Science 279:787–792

Belin T, Epron F (2005) Characterization methods of carbon nanotubes: a review. Mater Sci Eng B 119:105–118

Cao Q, Rogers JA (2010) Ultrathin films of single-walled carbon nanotubes for electronics and sensors: a review of fundamental and applied aspects. Adv Mater 21:29–53

Graupner R (2007) Raman spectroscopy of covalently functionalized single-wall carbon nanotubes. J Raman Spectrosc 38:673–683

Hong E, McKinstry ST, Smith R, Krishnaswamy SV, Freidhoff CB (2008) Vibration of micromachined circular piezoelectric diaphragms. IEEE Trans UFFC 53:697–706

Huang L, Jia Z, O'Brien S (2007) Orientated assembly of single-walled carbon nanotubes and applications. J Mater Chem 17: 3863–3874

Iijima S (1991) Helical microtubules of graphitic carbon. Nature 354: 56–58

Liu S, Yin Y, Cai C (2007) Immobilization and characterization of glucose oxidase on single-walled carbon nanotubes and its application to sensing glucose. Chin J Chem 25:439–447

Lourie O, Wagner HD (1998) Transmission electron microscopy observations of fracture of single-wall carbon nanotubes under axial tension. Appl Phys Lett 73:3527–3529

Lu M, Jang M-W, Haugstad G, Campbell SA, Cui TH (2009) Well-aligned and suspended single- walled carbon nanotube film: directed self-assembly, patterning, and characterization. Appl Phys Lett 94:261903

Meyer JC, Paillet M, Michel T, Moreac A, Neumann A, Duesberg GS, Roth S, Sauvajol J-L (2005) Raman modes of index-identified freestanding single-walled carbon nanotubes. Phys Rev Lett 95:217401–217404

Pop E, Mann D, Wang Q, Goodson K, Dai HJ (2006) Thermal conductance of an individual single-wall carbon nanotube above room temperature. Nano Lett 6:96–100

Treacy MMJ, Ebbesen TW, Gibson JM (1996) Exceptionally high Young's modulus observed for individual carbon nanotubes. Nature 381:678–680

Vosgueritchian M, Lemieux M, Dodge D, Bao Z (2010) Effect of surface chemistry on electronic properties of carbon nanotube network thin film transistors. ACS Nano 4:6137–6145

Yao Z, Kane CL, Dekker C (2000) High-field electrical transport in single-wall carbon nanotubes. Phys Rev Lett 84:2941–2944